August 27th, 2021

Star Formation Newsletter No.343 34-39

Shota Notsu (RIKEN)

-34: Long-term optical photometric monitoring of the FUor star V900 Mon
-35: Which molecule traces what: chemical diagnostics of protostellar sources
-36: Probing protoplanetary disk evolution in the Chamaeleon II region
-37: From downtown to the outskirts: a radio survey of the Orion Nebula Cluster
-38: Evidence of Accretion Burst: The Viscously Heated Inner Disk of the Embedded Protostar IRAS 16316-1540
-39: ALMA discovery of a dual dense probably rotating outflow from a massive young stellar object G18.88MME

https://arxiv.org/abs/2107.03696v2

35. Which molecule traces what: chemical diagnostics of protostellar sources

Łukasz Tychoniec, Ewine F. van Dishoeck, Merel L. R. van 't Hoff, Martijn L. van Gelder, Benoît Tabone, Yuan Chen, Daniel Harsono, Charles L. H. Hull, Michiel R. Hogerheijde, Nadia M. Murillo, John J. Tobin

The physical and chemical conditions in Class 0/I protostars are fundamental in unlocking the protostellar accretion process and its impact on planet formation. The aim is to determine which physical components are traced by different molecules at sub-arcsecond scales (100 - 400 au). We use a suite of Atacama Large Millimeter/submillimeter Array (ALMA) datasets in Band 6 (1 mm), Band 5 (1.8 mm) and Band 3 (3 mm) at spatial resolutions 0.5 - 3" for 16 protostellar sources. The protostellar envelope is well traced by $C^{18}O$, DCO^+ and N_2D^+, with the freeze-out of CO governing the chemistry at envelope scales. Molecular outflows are seen in classical shock tracers like SiO and SO, but ice-mantle products such as CH_3OH and HNCO released with the shock are also observed. The molecular jet is prominent not only in SiO and SO but also occasionally in H_2CO. The cavity walls show tracers of UV-irradiation such as C_2H c-C_3H_2 and CN. The hot inner envelope, apart from showing emission from complex organic molecules (COMs), also presents compact emission from small molecules like H_2S, SO, OCS and $H^{13}CN$, most likely related to ice sublimation and high-temperature chemistry. Sub-arcsecond millimeter-wave observations allow to identify those (simple) molecules that best trace each of the physical components of a protostellar system. COMs are found both in the hot inner envelope (high excitation lines) and in the outflows (lower-excitation lines) with comparable abundances. COMs can coexist with hydrocarbons in the same protostellar sources, but they trace different components. In the near future, mid-IR observations with JWST-MIRI will provide complementary information about the hottest gas and the ice mantle content, at unprecedented sensitivity and at resolutions comparable to ALMA for the same sources.

円盤+降着エンベロープ＋ジェット&アウトフロー等で構成されるClass 0/I原始星16天体に対し、ALMAで様々な分子輝線の観測(空間分解能: 0.5-3”)を実施。それぞれの物理構造をどの分子がトレースするかを調べた。

C_3H_2, CCH, ^{13}CS, CN →強いUV照射を受けるcavity-wallのトレーサー

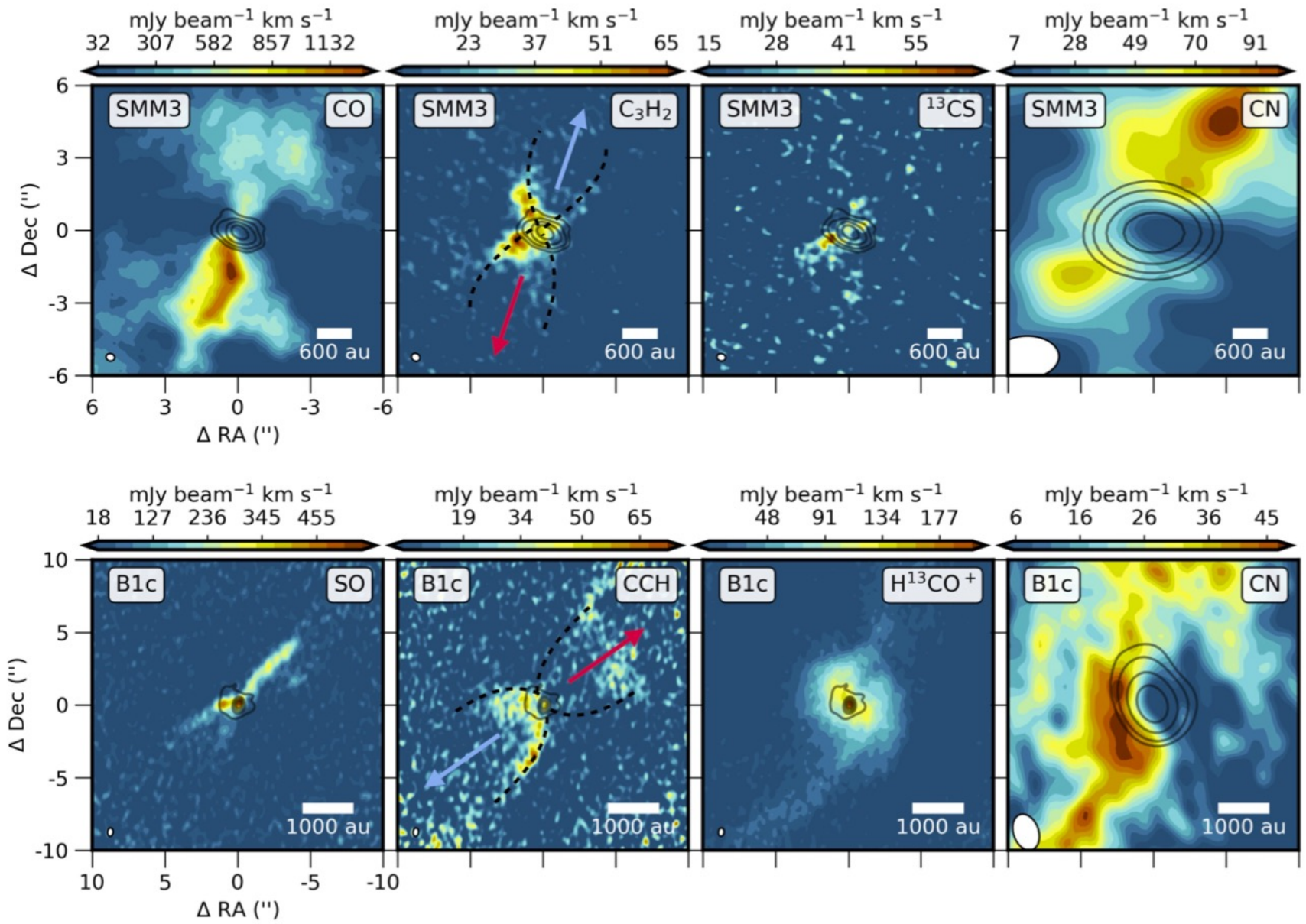

COMs (複雑な有機物)の観測結果

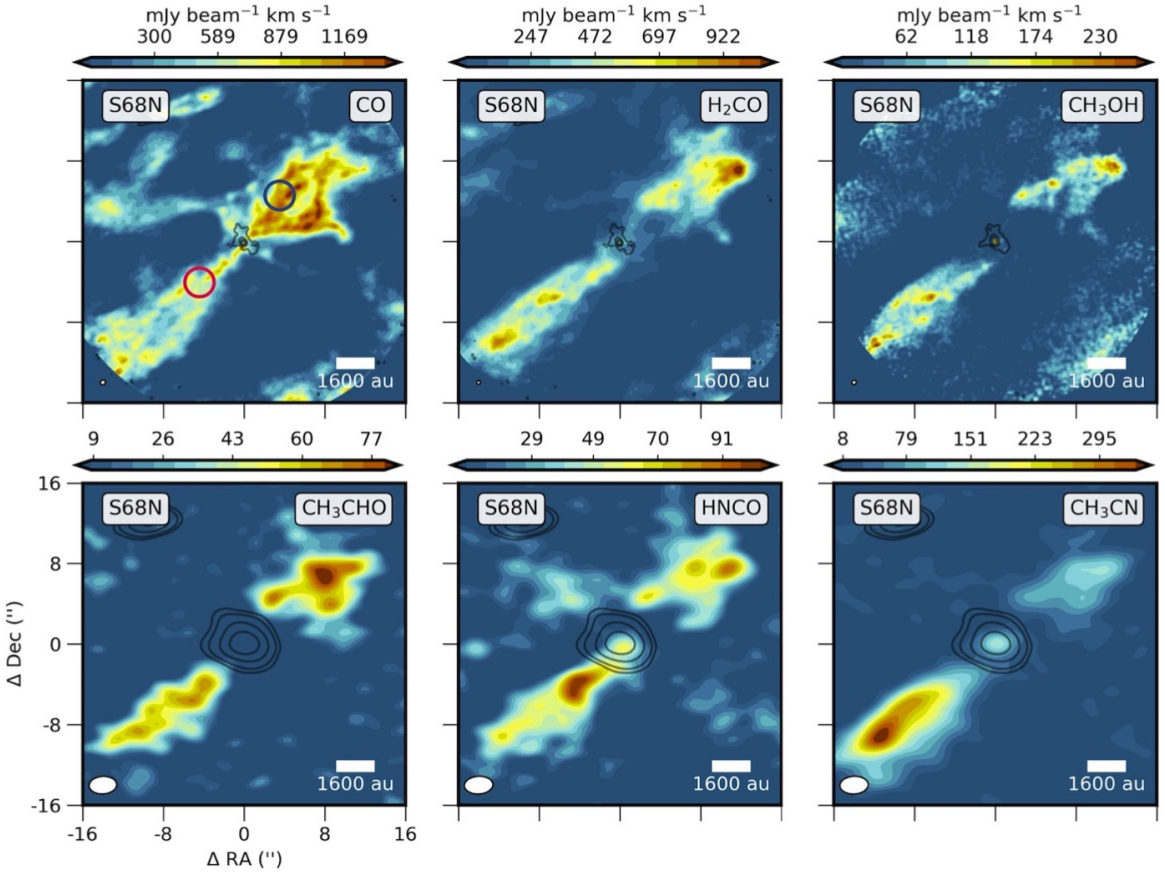

Fig. 6: Maps of the ice mantle tracers toward the S68N outflow, with the CO low-velocity outflow map for reference. *Top:* CO, H_2CO and CH_3OH moment 0 maps obtained in Band 6 at 0.″5 resolution. Circles show regions from which spectra were obtained for analysis in Section 7.1. *Bottom:* CH_3CHO, HNCO, and CH_3CN moment 0 maps obtained in Band 3 at 2.″5 resolution. The emission is integrated from -10 to -1 km s^{-1} and from 1 to 10 km s^{-1} w.r.t v_{sys}.

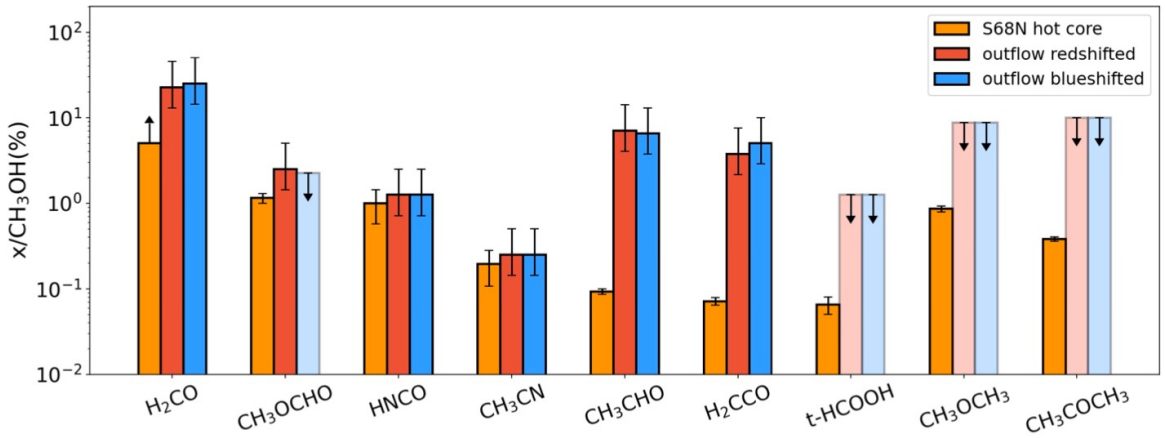

Fig. 13: Ratio of complex organic molecules with respect to CH_3OH in S68N. The ratios are shown for a 3″ region in both redshifted and blueshifted part of the outflow. The abundance ratios in the hot cores are taken from van Gelder et al. (2020) and Nazari et al. (2021). The errorbars mark the lower and upper limit on the ratios, as calculated from the optically thick CH_3OH emission (lower limit) and $^{13}CH_3OH$ (upper limit). All outflow abundances obtained from the Band 6 data at 0.″45 resolution except for CH_3OCHO and CH_3CN which were derived from Band 3 data at 3″.

Hot core (& warm disk): 高温領域(スノーライン内側)でダスト上から脱離したCOMsが存在
Outflow: 衝撃波面などでのsputtering でダスト上から叩き出されたCOMsが存在

$C^{18}O$, N_2D^+, DCO^+→Cold envelopesのトレーサー
H_2CS, OCS, COMs etc. → Inner warm envelopesのトレーサー

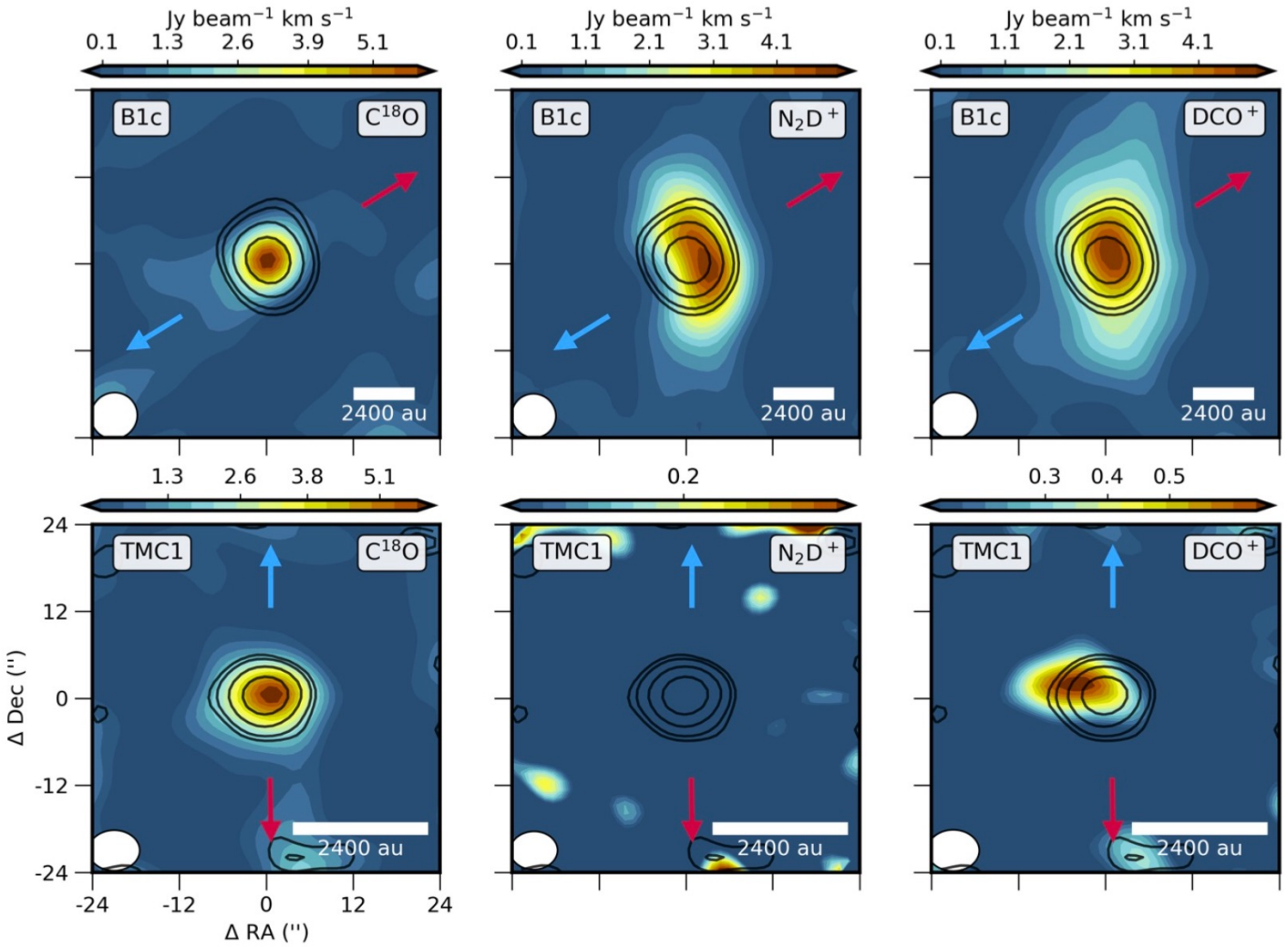

Fig. 2: Maps of key envelope tracers toward B1-c (Class 0, top) and TMC1 (Class I, bottom) obtained with ACA. Contours represent continuum emission at 1.3 mm observed with ACA. Note different distances to B1-c and TMC1 resulting in different spatial resolutions of the maps. *Left:* $C^{18}O$ 2 – 1 *Middle:* N_2D^+ 3 – 2. *Right:* DCO^+ 3 – 2. All moment 0 maps are integrated from -2.5 to 2.5 km s^{-1} w.r.t v_{sys}.

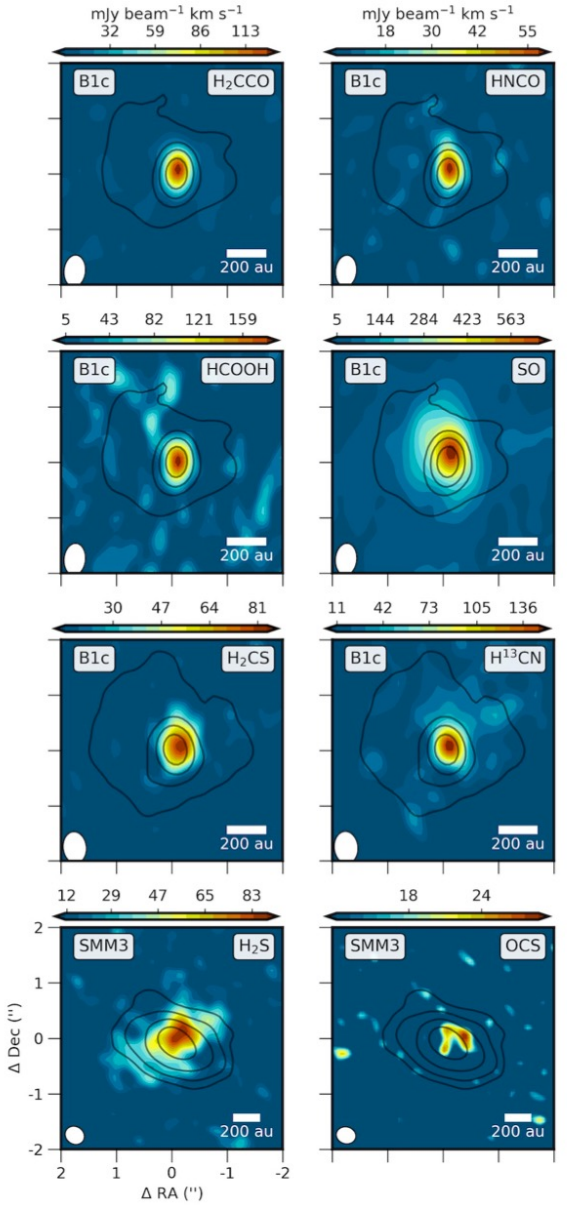

Fig. 9: Compact emission for B1-c and SMM3 for various molecules tracing the warm inner envelope (hot core). Moment 0 maps shown in colorscale integrated from -3 to 3 km s^{-1} w.r.t v_{sys}. 1.3 mm continuum presented in contours.

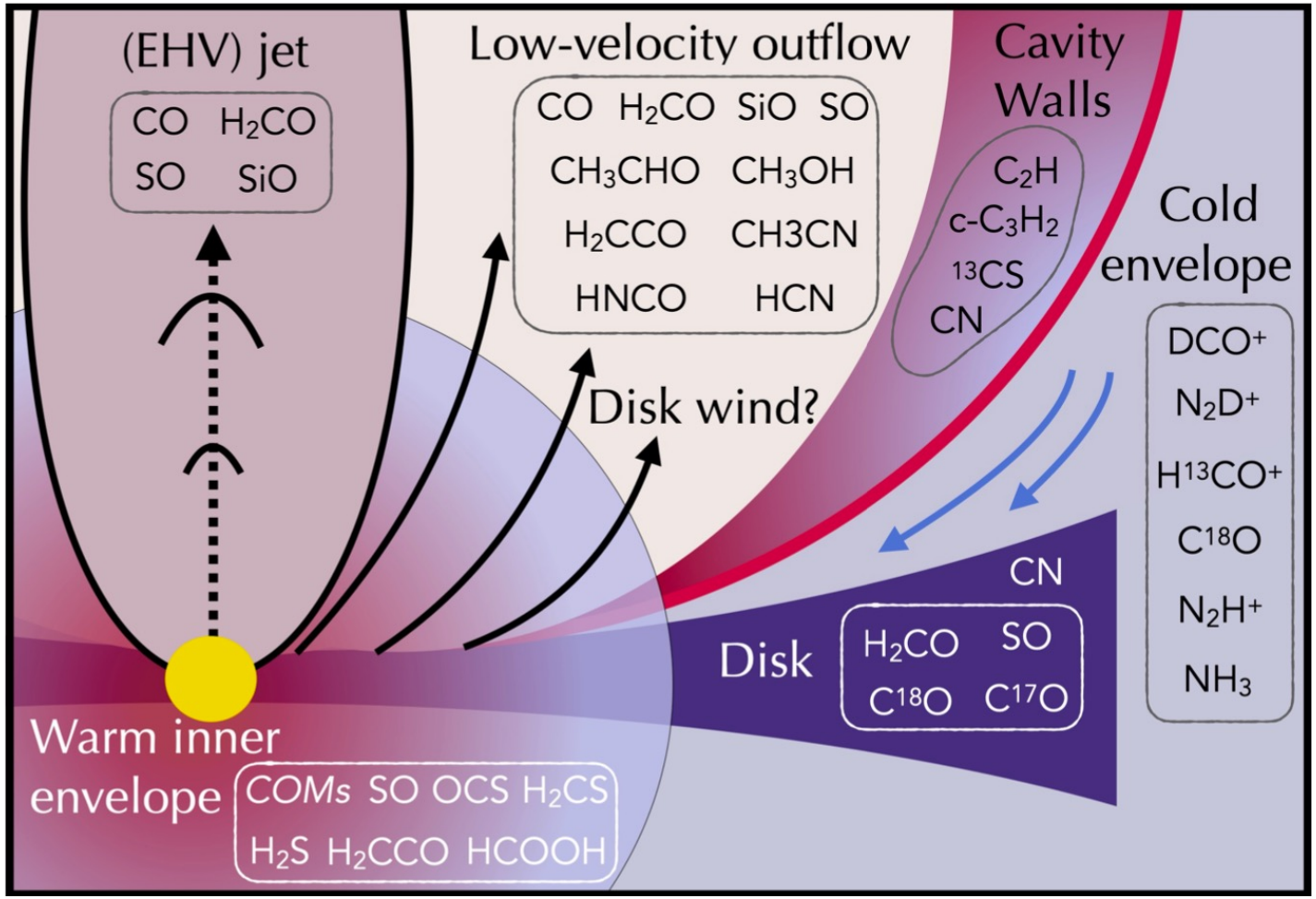

Fig. 11: Summary cartoon presenting key molecular tracers of different components, limited to molecules presented in this work except for NH_3 and N_2H^+ which are important large scale envelope tracers. CN molecule is shown on top of the disk as it traces the disk atmosphere and not the midplane. Protostar indicated in the center in yellow.

Table 2: Molecular tracers of physical components exclusive to this work

Molecule	Envelope	Disk	Hot core	Outflow	Jet	Cavity
CO	✓	—	—	✓	✓	✓
$C^{18}O$	✓	✓	—	✓	—	✓
^{13}CO	✓	✓	—	✓	—	✓
$C^{17}O$	✓	✓	✓	—	—	✓
$H^{13}CO^+$	✓	—	—	✓	—	✓
H_2CO	✓	✓	✓	✓	✓	—
H_2CS	—	✓	✓	—	—	—
SO	—	✓	✓	✓	✓	—
SiO	—	—	—	✓	✓	—
DCO^+	✓	—	—	—	—	—
N_2D^+	✓	—	—	—	—	—
OCS	—	—	✓	—	—	—
$O^{13}CS$	—	—	✓	—	—	—
HNCO	—	—	✓	✓	—	—
H_2CCO	—	—	✓	✓	—	—
HCOOH	—	—	✓	✓	—	—
^{13}CS	✓	—	—	—	—	✓
CN	✓	✓	—	—	—	✓
HCN	—	—	—	✓	—	—
$H^{13}CN$	—	—	✓	✓	—	—
C_2H	✓	—	—	✓	—	✓
$c\text{-}C_3H_2$	—	—	—	—	—	✓
CH_3CHO	—	—	✓	✓	—	—
CH_3CN	—	—	✓	✓	—	—
CH_3OCHO	—	—	✓	✓	—	—
CH_3OH	—	—	✓	✓	—	—
$^{13}CH_3OH$	—	—	✓	—	—	—

Table 3: Summary of evolution of chemical tracers

Component	Class 0	Class I
Envelope	Cold, dense envelope results in cold tracers (DCO^+, N_2H^+, N_2D^+)	Envelope dissipates, extent of cold tracers is much smaller
Jet	O-bearing molecules (CO, SiO, SO, H_2CO) are present in high-velocity bullets	Molecular jet disappears, seen only in atomic and ionised gas
Outflow	Ice sputtering (CH_3OH, HNCO) and grain destruction (SO, SiO) tracers are present	Decreased outflow mass and less dense envelope result in no tracers of sputtering and grain destruction, only faint CO remains
Cavity walls	Prominent signs of UV-irradiated cavity walls (CN, C_2H, c-C_3H_2)	No prominent signs of hydrocarbons in cavity walls, CN still present
Hot core	COMs and simple tracers of ice sublimation and high-temperature chemistry (H_2S, OCS)	Small extent plus disk shadowing results in less complexity, except for outbursting sources
Disk	Warm disk with COMs, dust obscuration	Colder disk molecules, Keplerian rotation seen in H_2CO, $C^{18}O$, CN in the disk surface.

Class 0 → Class I で円盤の寄与大、
円盤のサイズ増加&温度低下なども影響

https://arxiv.org/abs/2106.13847v1

36. Probing protoplanetary disk evolution in the Chamaeleon II region

M. Villenave, F. Menard, W. R. F. Dent, M. Benisty, G. van der Plas, J. P. Williams, M. Ansdell, A. Ribas, C. Caceres, H. Canovas, L. Cieza, A. Hales, I. Kamp, C. Pinte, D. A. Principe, M. R. Schreiber

Context. Characterizing the evolution of protoplanetary disks is necessary to improve our understanding of planet formation. Constraints on both dust and gas are needed to determine the dominant disk dissipation mechanisms. Aims. We aim to compare the disk dust masses in the Chamaeleon II (Cha II) star-forming region with other regions with ages between 1 and 10Myr. Methods. We use ALMA band 6 observations (1.3 mm) to survey 29 protoplanetary disks in Cha II. Dust mass estimates are derived from the continuum data. Results. Out of our initial sample of 29 disks, we detect 22 sources in the continuum, 10 in 12CO, 3 in 13CO, and none in C18O (J=2-1). Additionally, we detect two companion candidates in the continuum and 12CO emission. Most disk dust masses are lower than 10Mearth, assuming thermal emission from optically thin dust. We compare consistent estimations of the distributions of the disk dust mass and the disk-to-stellar mass ratios in Cha II with six other low mass and isolated star-forming regions in the age range of 1-10Myr: Upper Sco, CrA, IC 348, Cha I, Lupus, and Taurus. When comparing the dust-to-stellar mass ratio, we find that the masses of disks in Cha II are statistically different from those in Upper Sco and Taurus, and we confirm that disks in Upper Sco, the oldest region of the sample, are statistically less massive than in all other regions. Performing a second statistical test of the dust mass distributions from similar mass bins, we find no statistical differences between these regions and Cha II. Conclusions. We interpret these trends, most simply, as a sign of decline in the disk dust masses with time or dust evolution. Different global initial conditions in star-forming regions may also play a role, but their impact on the properties of a disk population is difficult to isolate in star-forming regions lacking nearby massive stars.

星形成領域Chamaeleon II (Cha II)の29天体に対してALMA観測を実施。円盤ダスト質量定量。
22天体でダスト連続波検出。得られた質量分布等を他の星形成領域のものと比較。

ダスト質量のmedian値: 4.5±1.5M_{earth}

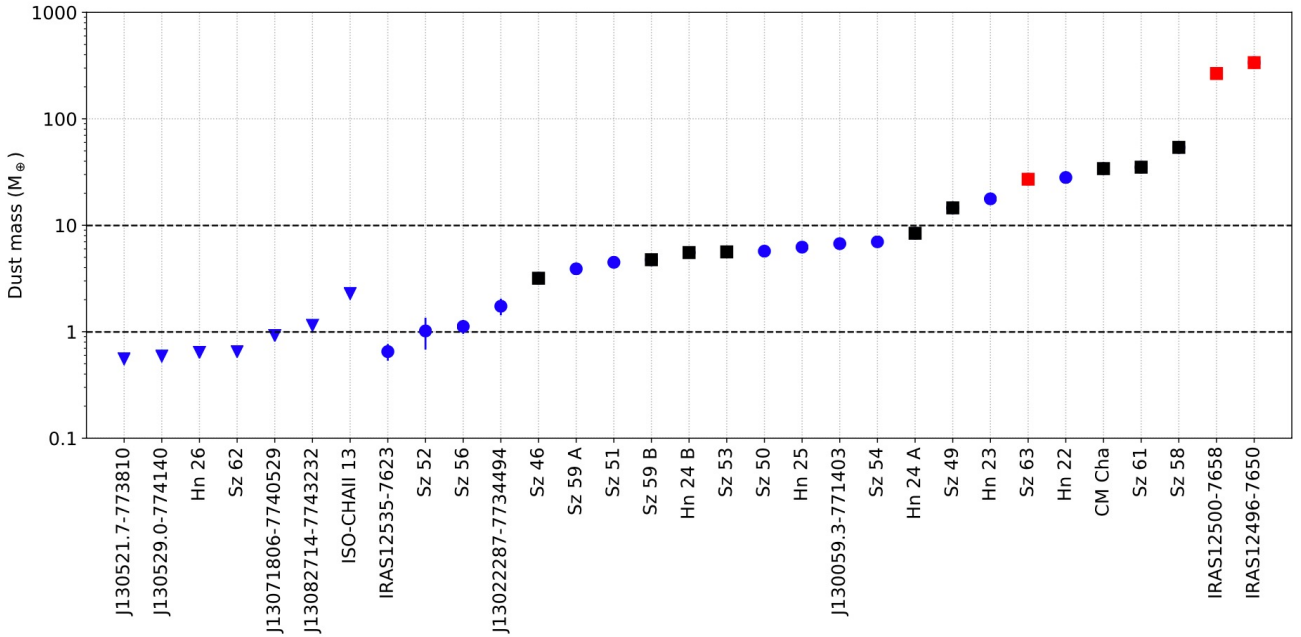

Fig. 3. Dust masses for the 31 sources in our Cha II sample expressed in Earth masses, ordered by increasing dust mass (Table 2). The black and red squares indicates the sources also detected in ^{12}CO and ^{13}CO, respectively. Round symbols show continuum only detected sources and the downward-facing triangles correspond to 3σ upper limits for non-detections.

$$M_{\rm dust} = \frac{F_\nu d^2}{\kappa_\nu B_\nu(T_{\rm dust})}.$$

Cha IIの年齢
4±2 Myr (古い値)
1-2 Myr (Gaia DR2に基づく値)

M_{dust}の分布(右上図): Taurusと比べCha IIは軽い天体が多い
Upper Sco (一番古い)は他の領域と比べ有意に軽い分布

年齢：1-10 Myr の星形成領域間の比較

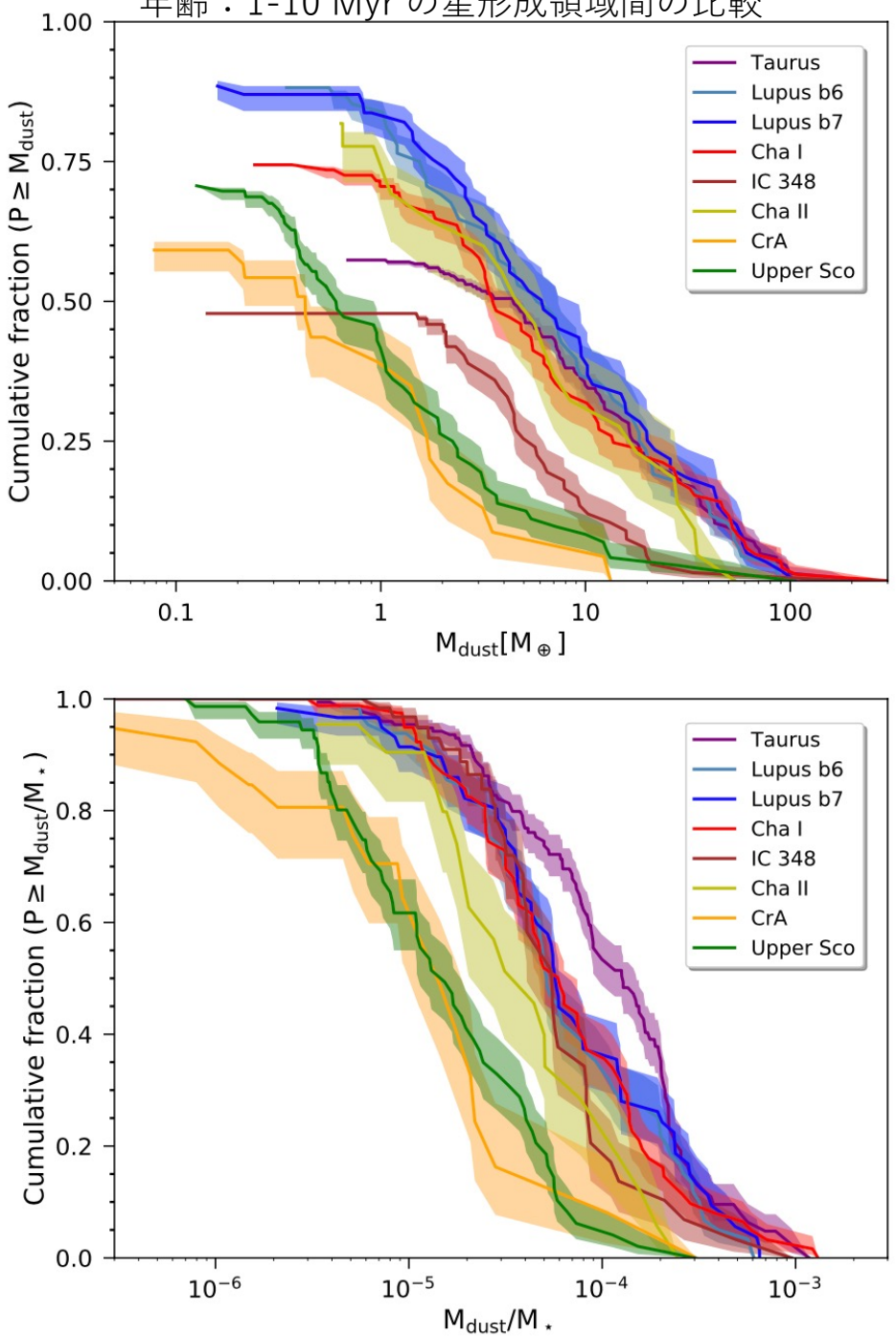

https://arxiv.org/abs/2106.13025v1

37. From downtown to the outskirts: a radio survey of the Orion Nebula Cluster

Jaime Vargas-González, Jan Forbrich, Sergio A. Dzib, John Bally

We present a newly enlarged census of the compact radio population towards the Orion Nebula Cluster (ONC) using high-sensitivity continuum maps (3-10 μJy bm^{-1}) from a total of $\sim$ 30 h centimeter-wavelength observations over an area of $\sim 20' \times 20'$ obtained in the C-band (4−8 GHz) with the Karl G. Jansky Very Large Array (VLA) in its high-resolution A-configuration. We thus complement our previous deep survey of the innermost areas of the ONC, now covering the field of view of the Chandra Orion Ultra-deep Project (COUP). Our catalog contains 521 compact radio sources of which 198 are new detections. Overall, we find that 17COUP sources have radio counterparts, while 53counterparts. Most notably, the radio detection fraction of X-ray sources is higher in the inner cluster and almost constant for $r > 3'$ (0.36 pc) from θ^1 Ori C suggesting a correlation between the radio emission mechanism of these sources and their distance from the most massive stars at the center of the cluster, for example due to increased photoionisation of circumstellar disks. The combination with our previous observations four years prior lead to the discovery of fast proper motions of up to $\sim$373 km s^{-1} from faint radio sources associated with ejecta of the OMC1 explosion. Finally, we search for strong radio variability. We found changes in flux density by a factor of $\lesssim$5 within our observations and a few sources with changes by a factor >10 on long timescales of a few years.

Orion Nebula Cluster (ONC)に対し新た高感度連続波サーベイをVLA C-band (4-8 GHz)で実施。
521個の電波源を同定。うち198個は 新検出。
Chandra Orion Ultra-deep Project (COUP)のX線源と比較すると、COUPの17%の天体は電波源があり、
電波源がある天体の53%はX線源があるという結果。
θ^1 Ori C (UV源として知られる大質量星)からの天体の空間分布などを議論。

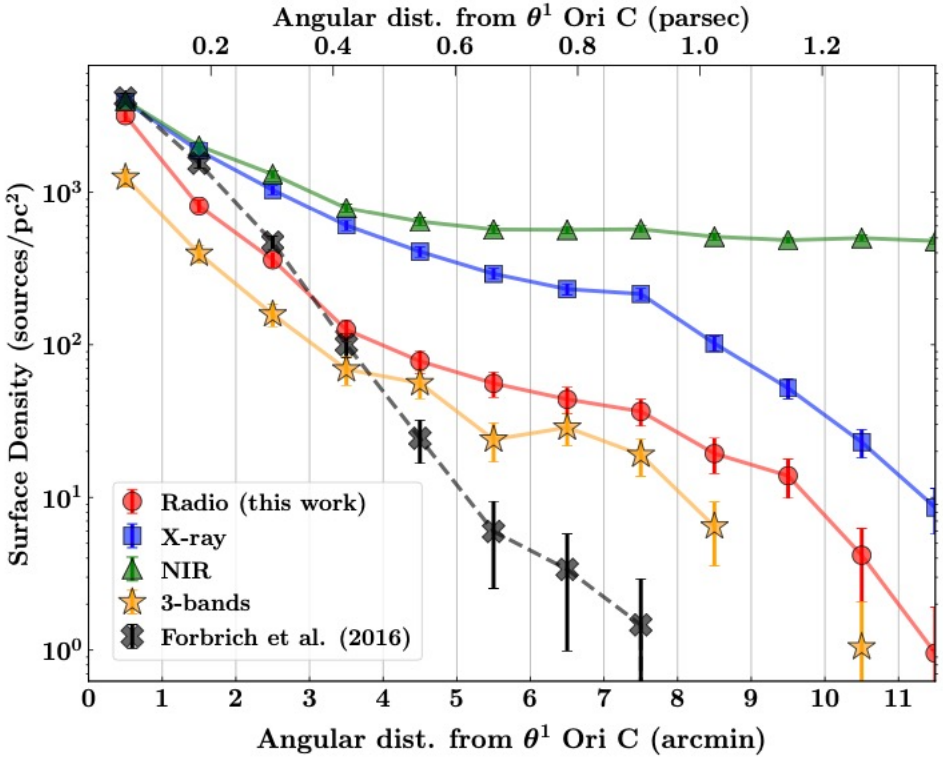

Figure 2. Azimuthally averaged surface number density as a function of projected distance to θ^1 Ori C for the three different wavelength populations. The VISION, COUP and radio catalogs are indicated by green, blue and red lines, respectively. Sources with detections in all three bands are indicated in orange line, while the dashed black lines indicate the distributions for the deep catalog from Forbrich et al. (2016). Each data point represent the surface density of sources within annular areas of 1′ width indicated by vertical lines and the error bars are based on error propagation from counting statistics (Poisson errors).

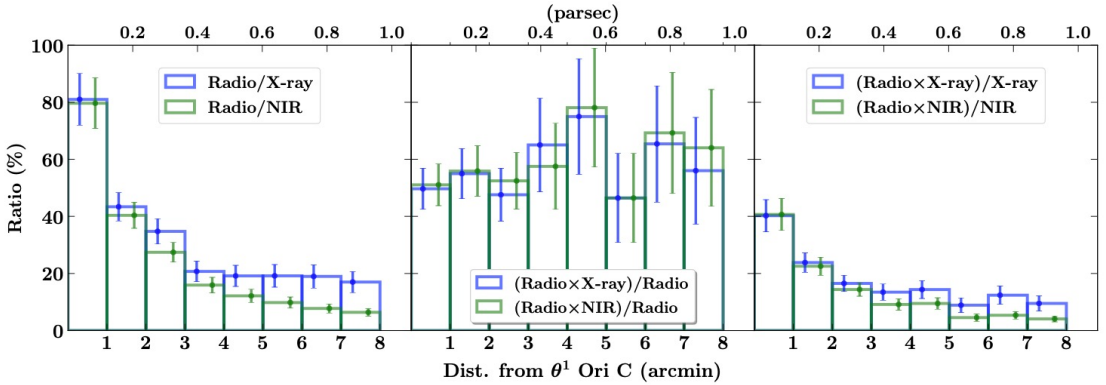

Figure 3. Detection fractions between the three different populations radio/X-ray/NIR as a function of distance to θ^1 Ori C. The left panel shows the fraction of radio sources over the X-ray (blue) and NIR (green) populations. Central panel shows the X-ray (blue) and NIR (green) detection fraction of radio sources. The right panel shows the radio detection fraction of X-ray sources (blue) and NIR sources (green). The 1σ error bars were derived from counting statistics (Poisson errors).

θ^1 Ori C (UV源として知られる大質量星)からの天体の空間分布

電波源はfree-free 放射など

電波源は<3”で距離に反比例
円盤のphotoionizationなどを反映?

https://arxiv.org/abs/2106.09626v1

39. ALMA discovery of a dual dense probably rotating outflow from a massive young stellar object G18.88MME

I. I. Zinchenko, L. K. Dewangan, T. Baug, D. K. Ojha, N. K. Bhadari

We report the discovery of a very dense jet-like fast molecular outflow surrounded by a wide-angle wind in a massive young stellar object (MYSO) G18.88MME (stellar mass ∼8 $M_\odot$) powering an Extended Green Object G18.89−0.47. Four cores MM1-4 are identified in the Atacama Large Millimeter/submillimeter Array (ALMA) 1.3 mm continuum map (resolution ∼0.”8) toward G18.88MME, and are seen at the center of the emission structure (extent ∼0.3 pc × 0.2 pc) detected in the ALMA map. G18.88MME is embedded in the core MM1 (mass ∼13-18 $M_\odot$), where no radio continuum emission is detected. The molecular outflow centered at MM1 is investigated in the SiO(5-4), HC_3N(24-23) and ^{13}CO(2-1) lines. The detection of HC_3N in the outflow is rare in MYSOs and indicates its very high density. The position-velocity diagrams display a fast narrow outflow (extent ∼28000 AU) and a slower wide-angle more extended outflow toward MM1, and both of these components show a transverse velocity gradient indicative of a possible rotation. All these observed features together make G18.88MME as a unique object for studying the unification of the jet-driven and wind-driven scenarios of molecular outflows in MYSOs.

ALMA観測を通じ、大質量原始星 G18.88MME (8太陽質量星)でのjet-likeな分子アウトフローを発見。
SiO(5–4), HC_3N(24–23), ^{13}CO(2–1) の輝線を検出。
HC_3Nが検出されていることで、高密度なアウトフローを示唆

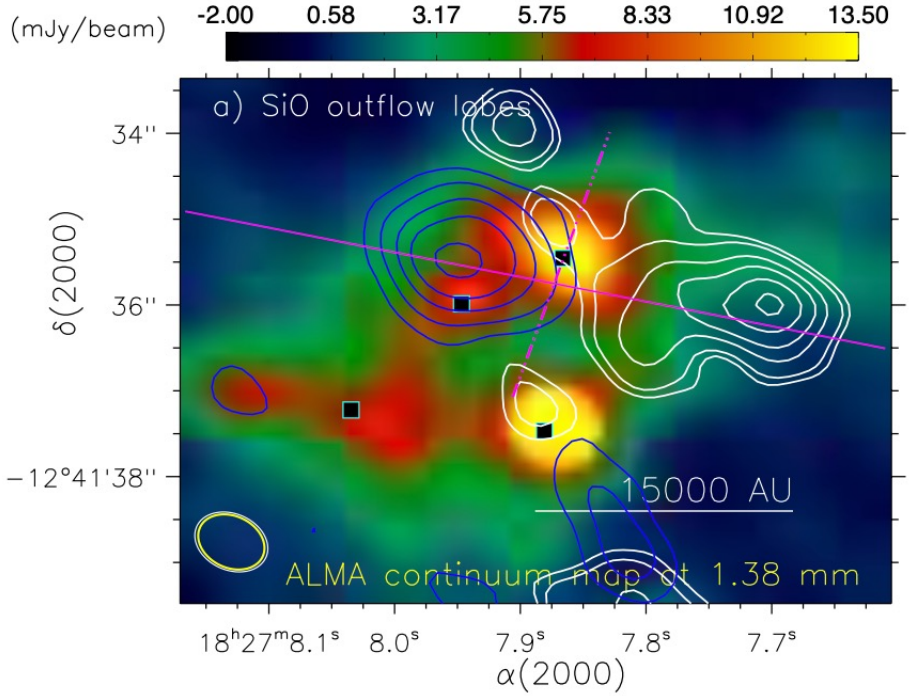

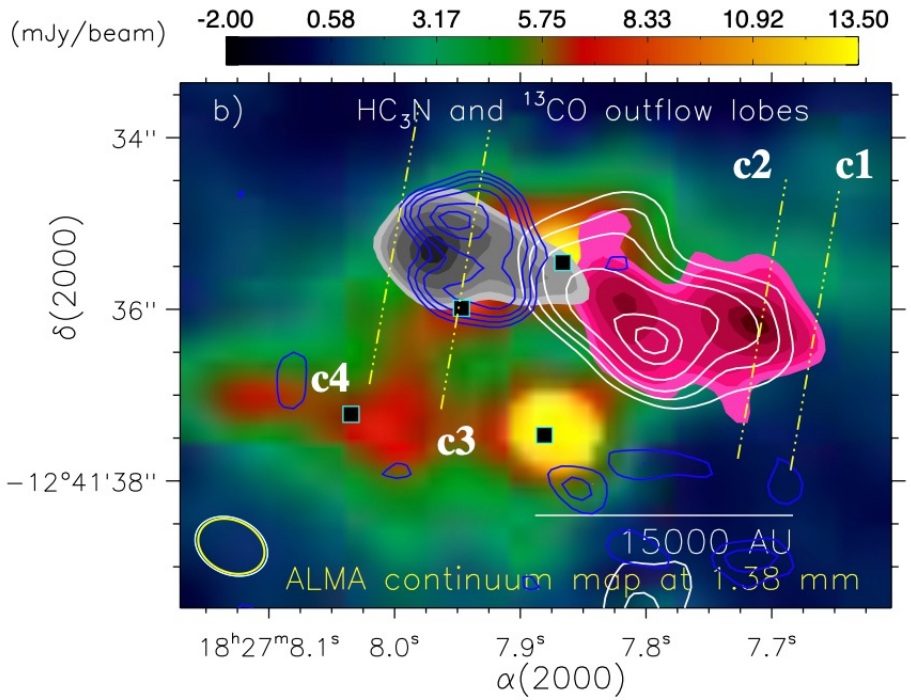

Solid curves: ^{13}CO
Filled: H^{13}CN

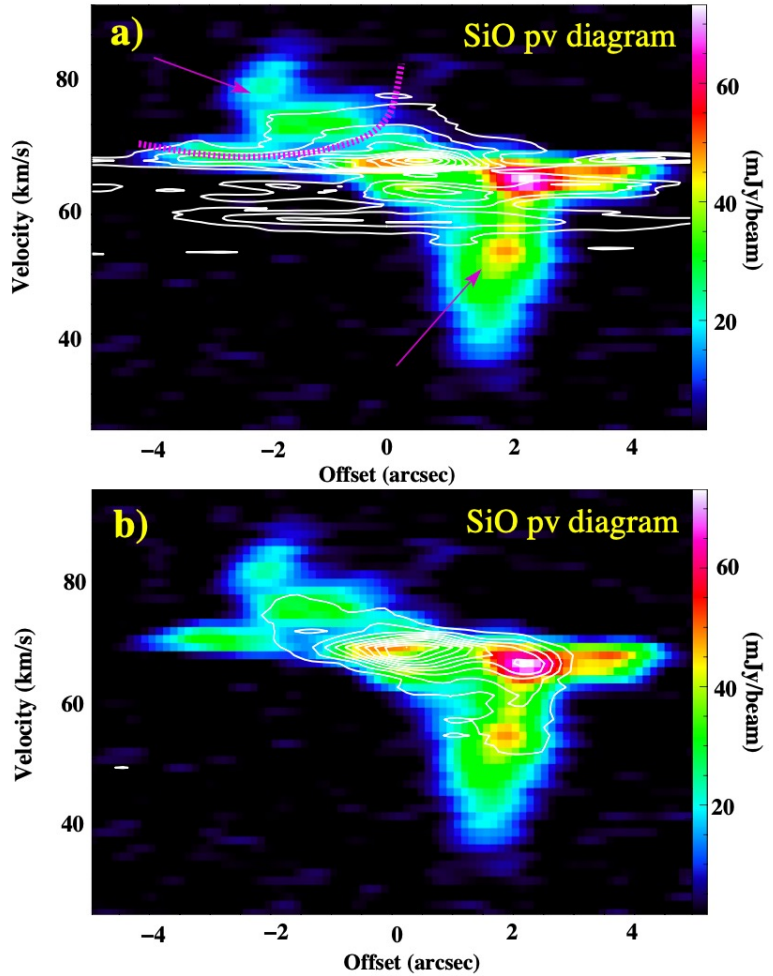

Figure 5. a) PV diagram in the SiO line at the PA of 81° across "MM1" (see a solid line in Figure 3a). The contours show the ^{13}CO emission. The contour levels are at (0.05, 0.15, ..., 0.95) × 456 mJy beam^{-1}. The arrows indicate the jet-like outflow and the dashed curve indicates the probable wide-angle wind. b) Overlay of HC_3N PV contours on the PV diagram in the SiO line. The contour levels are at (0.1, 0.2, ..., 0.9) × 69 mJy beam^{-1}.

https://arxiv.org/abs/2105.14906v1

34. Long-term optical photometric monitoring of the FUor star V900 Mon

Evgeni Semkov, Stoyanka Peneva, Sunay Ibryamov

We present results from photometric monitoring of V900 Mon, one of the newly discovered and still under-studied object from FU Orionis type. FUor phenomenon is very rarely observed, but it is essential for stellar evolution. Since we only know about twenty stars of this type, the study of each new object is very important for our knowledge. Our data was obtained in the optical spectral region with BVRI Johnson-Cousins set of filters during the period from September 2011 to April 2021. In order to follow the photometric history of the object, we measured its stellar magnitudes on the available plates from the Mikulski Archive for Space Telescopes. The collected archival data suggests that the rise in brightness of V900 Mon began after January 1989 and the outburst goes so far. In November 2009, when the outburst was registered, the star had already reached a level of brightness close to the current one. Our observations indicate that during the period 2011-2017 the stellar magnitude increased gradually in each pass band. The observed amplitude of the outburst is about 4 magnitudes (R). During the last three years, the increase in brightness has stopped and there has even been a slight decline. The comparison of the light curves of the known FUor objects shows that they are very diverse and are rarely repeated. However, the photometric data we have so far shows that the V900 Mon's light curve is somewhat similar to this of V1515 Cyg and V733 Cep.

FU Ori型星 V900 Monの10年間にわたる可視光(B, V, R, I バンド)測光モニター観測のデータを解析。
この天体では1989年以降、Rバンドの振幅で4桁も増光したアウトバースト現象が続いている。
今回解析した2011年9月以降のデータの中では、2017年から2018年の期間に最大の明るさが観測され、
その後、明るさの低下が始まった。

https://arxiv.org/abs/2106.15804v1

38. **Evidence of Accretion Burst: The Viscously Heated Inner Disk of the Embedded Protostar IRAS 16316-1540**

Sung-Yong Yoon, Jeong-Eun Lee, Seokho Lee, Gregory J. Herczeg, Sunkyung Park, Gregory N. Mace, Jae-Joon Lee, Daniel T. Jaffe

Outbursts of young stellar objects occur when the mass accretion rate suddenly increases. However, such outbursts are difficult to detect for deeply embedded protostars due to their thick envelope and the rarity of outbursts. The near-IR spectroscopy is a useful tool to identify ongoing outburst candidates by the characteristic absorption features that indicate a disk origin. However, without high-resolution spectroscopy, the spectra of outburst candidates can be confused with the late-type stars since they have similar spectral features. For the protostar IRAS 16316-1540, the near-IR spectrum has line equivalent widths that are consistent with M-dwarf photospheres. However, our high-resolution IGRINS spectra reveal that the absorption lines have boxy and/or double-peaked profiles, as expected from a disk and not the star. The continuum emission source is likely the hot, optically thick disk, heated by viscous accretion. The projected disk rotation velocity of 41±5 km s^{-1} corresponds to ∼ 0.1 AU. Based on the result, we suggest IRAS 16316-1540 as an ongoing outburst candidate. Viscous heating of disks is usually interpreted as evidence for ongoing bursts, which may be more common than previously estimated from low-resolution near-IR spectra.

近赤外線高分散分光観測を通じ吸収線の形状を調べる事で、埋もれた原始星のアウトバースト現象の探索が可能
本研究では、原始星 IRAS16316-1540の近赤外高分散分光観測を実施。Double peak profileから0.1 auのKepler回転に相当する速度を算出。
→粘性加熱で温められたガスからの放射を捉えていて、アウトバースト現象が進行中。